A Combined Method for Determining Inhibition Type, Kinetic Parameters, and Inhibition Coefficients for Aerobic Cometabolism of 1,1,1-Trichloroethane by a Butane-Grown Mixed Culture

Young Kim,[1] Daniel J. Arp,[2] Lewis Semprini[1]

[1]Department of Civil, Construction, and Environmental Engineering, Oregon State University, Corvallis, Oregon 97331-2302; e-mail: lewis.semprini@orst.edu
[2]Department of Botany and Plant Pathology, Oregon State University, Corvallis, Oregon 97331

Received 12 April 2001; accepted 25 September 2001

Published online 9 January 2002

Abstract: A combined method for determining inhibition type, kinetic parameters, and inhibition coefficients is developed and presented. The method was validated by applying it to data obtained from batch kinetics of the aerobic cometabolism of 1,1,1-trichloroethane (1,1,1-TCA) by a butane-grown mixed culture. The maximum degradation rates (k_{max}) and half-saturation coefficients (K_s) were independently determined in single compound tests, and compared with those obtained from inhibition tests. The inhibition type was determined using direct linear plots at various substrate and inhibitor concentrations. Kinetic parameters (k_{max} and K_s) and inhibition coefficients (K_{ic} and K_{iu}) were determined by nonlinear least squares regression (NLSR) fits of the inhibition model determined from the direct linear plots. Initial guesses of the kinetic parameters for NLSR were determined from linearized inhibition equations that were derived from the correlations between apparent maximum degradation rates (k_{max}^{app}) and/or the apparent half-saturation coefficient (K_s^{app}) and the k_{max}, K_s, and inhibitor concentration (I_L) for each inhibition equation. Two different inhibition types were indicated from the direct linear plots: competitive inhibition of 1,1,1-TCA on butane degradation, and mixed inhibition of 1,1,1-TCA transformation by butane. Good agreement was achieved between independently measured k_{max} and K_s values and those obtained from both NLSR and the linearized inhibition equations. The initial guesses of all the kinetic parameters determined from linear plots were in the range of the values estimated from NLSR analysis. Overall the results show that use of the direct linear plot method to identify the inhibition type, coupled with initial guesses from linearized plots for NLSR analysis, results in an accurate method for determining inhibition types and coefficients. Detailed studies with pure cultures and purified enzymes are needed to further demonstrate the utility of this method. *Biotechnol Bioeng* **77**: 564–576, 2002; DOI 10.1002/bit.10145

Correspondence to: L. Semprini

Contract grant sponsor: Western Region Hazardous Substance Research Center, U.S. Environmental Protection Agency
Contract grant number: R-815738.

Keywords: direct linear plot; linearized inhibition equations; nonlinear least squares regression; inhibition type; kinetic parameters; aerobic cometabolism of 1,1,1-trichloroethane

INTRODUCTION

Competitive inhibition is an important process to consider in the aerobic cometabolism of chlorinated aliphatic hydrocarbons (CAHs), because there is competition between CAH and growth substrate for enzyme active sites due to lack of enzyme specificity. Competitive inhibition during aerobic cometabolism has been most widely proposed and successfully modeled with methane oxidizers, *Nitrosomonas europaea*, and *Pseudomonas cepacia* G4 (Anderson and McCarty, 1994, 1996; Chang and Alvarez-Cohen, 1995; Chang and Criddle, 1997; Ely et al., 1997; Landa et al., 1994). However, different inhibition types have also been observed. Keener and Arp (1993) reported noncompetitive inhibition of chloromethane and chloroethane and competitive inhibition of methane and ethylene on NH_4^+-dependent NO_2^- production by *N. europaea*. Keenan and co-workers (1994) reported that propane inhibition of trichloroethylene (TCE) transformation by a propane-oxidizing enrichment culture was best fit by a noncompetitive inhibition model. However, studies to determine the inhibition type between the growth substrate and the CAH are limited.

Convenient linearized plots, especially Lineweaver-Burk plot, have been widely used to determine the inhibition type and to estimate kinetic parameters for the aerobic cometabolism of CAHs (Alvarez-Cohen and McCarty, 1991; Chang and Alvarez-Cohen, 1995, 1996, 1997; Keener and Arp, 1993). Visual determination of inhibition type and the estimation of kinetic parameters from classical linear plotting are not straightforward as

discussed by many researchers (Dowd and Riggs, 1965; Eisenthal and Cornish-Bowden, 1974; Robinson, 1985; Robinson and Charaklis, 1984).

Here we present a combined method for determining the inhibition type, the kinetic parameters, and the inhibition coefficients. The direct linear plot method of Eisenthal and Cornish-Bowden (1974) was used to determine the inhibition type. This method has several advantages over other convenient linearized plots, such as Lineweaver-Burk and Hanse plot. The main advantage is that data inversion is not required. With linear regression methods, outliers can dramatically affect kinetic parameter estimates. However, the direct linear plot method is less sensitive to outliers, because the best estimate is the median rather than the mean. Nonlinear least squares regression (NLSR) analysis has been shown to be a better method for estimating the kinetic parameters than the convenient linearized plots (Robinson, 1985; Robinson and Charaklis, 1984). However, distinguishing between inhibition models can be problematic when using NLSR, and fairly accurate initial guesses of parameters are required. This study presents a combined method, both direct linear plots to identify the inhibition type and NLSR analysis to estimate the kinetic parameters, using graphically estimated kinetic parameters as initial guesses, for evaluating kinetic parameters, inhibition types, and inhibition coefficients.

Laboratory and field studies have shown that 1,1,1-trichloroethane (1,1,1-TCA), which is one of major CAH-contaminants in groundwater is difficult to treat through aerobic cometabolism. Only slow rates of 1,1,1-TCA transformation were observed in the laboratory with *Methylosinus trichosporium* OB3b and its mutant (Aziz et al., 1999; Oldenhuis et al., 1991). During in situ studies with methane-utilizing microorganisms (Semprini et al., 1990) or with phenol utilizing microorganisms (Hopkins et al., 1993; Hopkins and McCarty, 1995), 1,1,1-TCA was not transformed, despite effective transformation of chlorinated ethenes. In our previous studies with resting cells, a butane-grown mixed culture effectively transformed 1,1,1-TCA (Kim et al., 2000). For example, the culture had a greater ability to transform 1,1,1-TCA than a methane-grown mixed culture on the basis of amount transformed per unit mass cells (Chang and Alvarez-Cohen, 1996). Thus, the method was applied to inhibition kinetic studies of 1,1,1-TCA transformations with this butane-grown culture.

MATERIALS AND METHODS

A Butane-Utilizing Mixed Culture

The butane-utilizing enrichment was obtained from Hanford soil microcosms and grown in batch incubations described by Kim et al. (1997, 2000). To obtain a reproducible inoculum for the kinetic tests, the cells grown in media were washed, and cell suspensions (1 mL) were transferred to autoclaved 2-mL cryogenic vials (Nalgene Company, Rochester, NY), containing 70 μL of dimethyl sulfoxide (DMSO). The vials were stored in liquid nitrogen. Over the course of the kinetic tests the stored cells were used as the inoculum for batch-grown cells. This method of storing cells showed stable activity in methanotrophic studies (Anderson and McCarty, 1996, 1997) and in our studies.

To grow cells for the batch kinetic tests, the frozen cells were thawed, washed, and resuspended three times to remove DMSO and grown in batch growth reactors on 10% butane (vol/vol) in air. The cells (250 mL) were incubated in the dark at 30°C on a rotary table at 210 rpm, and harvested at OD_{600} of 0.6. The cells were concentrated by three cycles of centrifuging (6,000 × g for 15 minutes), washing, and resuspending in media. Based on butane uptake activity, resting cell activity was stable for 10 hours after harvesting. Thus, all kinetic tests were performed within 10 hours of harvesting the cells.

Chemicals

Butane (≥99%) was purchased from AIRCO (Vancouver, WA). 1,1,1-TCA (99.5% anhydrous) was purchased from Aldrich Chemical Co. (Milwaukee, WI). A saturated aqueous stock solution of 1,1,1-TCA was prepared at 20°C by adding specific amounts of the pure liquid compound to 125-mL serum bottles containing autoclaved deionized water. This procedure eliminated the use of carrier solvents, such as methanol. The bottles were shaken for 6 hours prior to use to ensure saturation, and then allowed to settle for 6 hours before use. Butane was volumetrically transferred to the batch bottles using gastight syringes (Precision Sampling Corp., Baton Rouge, LA).

Batch Experiments

Batch kinetic studies were performed at 20°C in 26-mL glass serum vials. Mineral medium (4.5 mL) described by Kim et al. (2000) was added to vials, and the remaining volume (21.5 mL) was filled with air. The vials were then crimp sealed with Teflon-lined rubber septa (Kimble, Vineland, NJ). No external energy source was added. The tests, therefore, relied on the internal energy reserves to drive 1,1,1-TCA transformation as described by Kim et al. (2000).

A volumetric amount of saturated aqueous stock solution of 1,1,1-TCA or butane or both was added into the vials to achieve desired initial aqueous concentrations. The vials were shaken on a rotary shaker at 260 rpm to equilibrate to 20°C. The initial headspace concentration was measured prior to adding the cells to initiate the transformation reaction. After cell addition, the bottles were vigorously hand-shaken for 10 seconds, and then placed on a rotary shaker operated at 260 rpm.

Mass transfer experiments were performed to assure that the equilibrium assumption was valid over the time scale of the kinetic experiments at this shaking speed (Kim, 2000). Headspace concentrations were measured at five equally spaced time intervals over a period of approximately 20 min. The headspace concentrations were converted into total mass in the reaction vial based on mass balance, and then initial transformation/degradation rates were determined by applying linear regression on the data. An example set of data and corresponding linear regression for 1,1,1-TCA inhibition of butane utilization are shown in Figure 1.

Measuring an accurate initial rate of CAH transformation is difficult, because CAHs are transformed with finite capacity due to transformation product toxicity and energy limitations. Therefore, maintaining a low ratio of the amount of CAH transformed to initial cell mass compared to the finite capacity is important to obtain accurate initial rates of CAH transformation. Based on our previous results (Kim et al., 2000), the amount of 1,1,1-TCA transformed per cell mass over 30 hours was 0.33 μmol/mg total suspended solids (TSS), and the initial transformation rate of 1,1,1-TCA was not greatly affected at less than 30% of this value. For the kinetic studies reported here, the amount of 1,1,1-TCA ultimately transformed per milligram TSS over the test period ranged from 5 to 21% of the value. Thus, the ratio of the amount of 1,1,1-TCA transformed to mass of cells added was low enough so the loss in cell activity resulting from 1,1,1-TCA transformation was minimal, and thus did not affect the transformation rate.

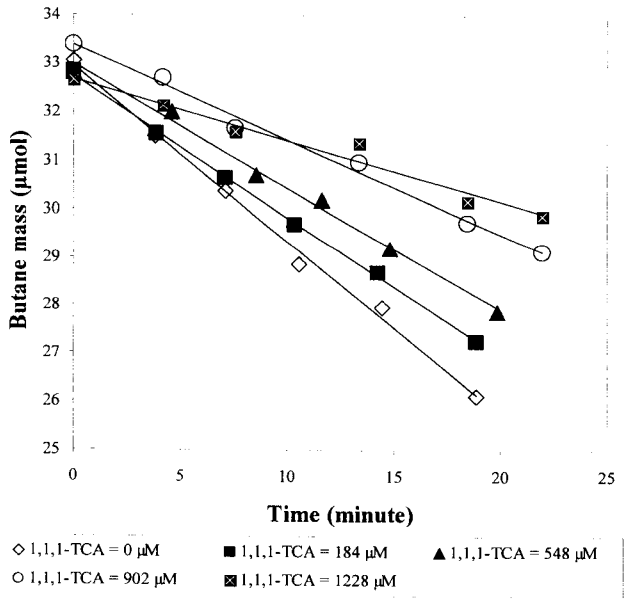

Figure 1. Determining initial rates of butane degradation by measured temporal butane masses remaining in the presence of various concentrations of 1,1,1-TCA (inhibitor), cell mass added (10.8 mg TSS) and applying linear regression on the data. Average initial butane mass (±95% confidence interval) was 33 ± 0.3 μmol, corresponding to average aqueous butane concentration of 40 ± 0.3 μ*M*.

Procedures for performing inhibition studies followed the batch kinetic test method described by Cornish-Bowden (1994). For single substrate kinetic tests to determine k_{max} and K_s values, triplicate vials were prepared at each of 10 different substrate concentrations. Preliminary inhibition experiments were performed to determine the range of concentrations of an inhibitor (a substance that decreases the rate of substrate degradation when present in the reaction mixture) and a substrate (a substance the reaction rate of which is decreased when an inhibitor is present in the reaction mixture) to be used in the studies.

Acetylene Inactivation Experiment

To investigate the kinetic diversity of the butane monooxygenase enzyme in the mixed culture, enzyme inactivation studies as described by Silverman (1988) were conducted. An experiment to evaluate the loss of butane uptake activity on exposure to acetylene, a mechanism-based inactivator (suicide substrate) of methane, ammonia, and butane monooxygenases (Hamamura et al., 1999; Keener et al., 1998; Prior and Daltan, 1985), was performed. The loss in activity as a function of time was used to determine the monooxygenase diversity of the butane-grown mixed culture.

To measure a time-dependent loss of butane uptake activity on exposure to acetylene, 100 μL-acetylene (0.33% vol/vol in headspace) was added into the 50-mL gas tight syringe (Unimetrics No 7450, Folsom, CA) containing cell suspension in media (20 mL) and air (30 mL). The syringe was sealed and hand-shaken throughout the experiment. Samples of the acetylene-treated cell suspension (1.5 mL) were taken as a function of time from the 50-mL gas tight syringe using 5-mL syringes. The acetylene was removed from the samples by equilibrating with air and removing air. The 1-mL cell suspensions were added into 26-mL batch bottles containing growth media (3 mL), butane (0.5 mL pure butane), and headspace air (22 mL). Initial butane degradation rates were measured as described above.

Analysis

The gaseous concentrations of butane and 1,1,1-TCA were determined by analysis of the serum vials headspace. The compound's masses in the test bottle were calculated, using the headspace and aqueous volumes and published Henry's constants (Gossett, 1987; Mackay and Shiu, 1981). Calibration curves for the compounds were developed using external standards. Headspace concentrations of the compounds were determined by injecting 100 μL of the headspace sample into a HP5890 series gas chromatograph (GC) connected to a photoionization detector (PID), followed by a flame ionization detector (FID) at 250°C. The GC was operated at the following conditions: oven temperature, 190°C; carrier

gas (He) flow, 15 mL/min; H_2 flow to detectors, 35 mL/min; airflow to detectors, 165 mL/min; and FID detector makeup gas (He) flow, 15 mL/min. Chromatographic separation was performed with a 30-m megabore GSQ-PLOT column from J&W Scientific (Folsom, CA).

Culture density was determined as TSS (American Public Health Association, 1985), using 0.1-μm membrane filter (Micro Separation Inc., Westboro, MA). The OD_{600} of cultures was measured using an HP8453 UV-visible spectrophotometer.

A COMBINED METHOD FOR DETERMINING INHIBITION TYPE AND KINETIC PARAMETERS

Inhibition Types

For batch kinetic and inhibition studies the Michaelis-Menten equation can be modified to include a mass balance between the air and aqueous phase, assuming equilibrium partitioning. Mass transfer experiments were performed to assure that the equilibrium assumption was valid over the time scale of the kinetic experiments (Kim, 2000). The modified Michaelis-Menten equation for a substrate and the substrate concentration in the liquid phase are provided in Eqs. (1), (2), and (3),

$$v = \frac{-k_{\max}^{app} S_L}{K_s^{app} + S_L} \tag{1}$$

$$S_L = \left(\frac{M_s}{V_L + V_G H_{cs}}\right) \tag{2}$$

$$v = \frac{-k_{\max}^{app}\left(\frac{M_s}{V_L+V_G H_{cs}}\right)}{K_s^{app} + \left(\frac{M_s}{V_L+V_G H_{cs}}\right)} \tag{3}$$

where v is specific substrate degradation rate (μmol/mg TSS/h), and $k_{\max}^{app}$ and K_s^{app} are the apparent values of k_{max} and K_s in the presence of inhibitor, respectively. Thus, $k_{\max}^{app}$ and K_s^{app} are equal to k_{max} and K_s, respectively, in the absence of inhibitor. S_L is the substrate concentration in liquid phase (μM), M_s is the total substrate mass in bottle (μmol), H_{cs} is the dimensionless Henry's constant of substrate, V_L is the volume of liquid phase (L), and V_G is the volume of gas phase (L).

For each of the four inhibition types—competitive, uncompetitive, mixed, and noncompetitive inhibition (Cornish-Bowden, 1994)—the inhibition model equation can be written by substituting $k_{\max}^{app}$ and K_s^{app} as presented in Table I into Eq. (1). In Table I, K_{ic} and K_{iu} are inhibition coefficients (μM), and I_L is an inhibitor concentration in liquid phase (μM) expressed by Eq. (4),

$$I_L = \left(\frac{M_i}{V_L + V_G H_{ci}}\right) \tag{4}$$

where M_i is total mass of inhibitor in bottle (μmol) and H_{ci} is a Henry's constant of an inhibitor. For purified enzymes with one substrate and an unreactive inhibitor, K_{ic} and K_{iu} are the equilibrium constants for inhibitor binding to the free enzyme (E) and the enzyme-substrate complex (ES), respectively (Cornish-Bowden, 1994). We assume that the kinetics for purified enzymes can be applied to whole cells.

Table I also presents how $k_{\max}^{app}$ and K_s^{app} vary with increasing I_L concentration. Each inhibition shows different $k_{\max}^{app}$ or K_s^{app} or both with increasing I_L concentration. A competitive inhibitor does not affect k_{max}, whereas k_{max} approaches zero with increasing concentrations of the other inhibitor types. The variation of K_s^{app} is different with different inhibition types. The variation patterns of both parameters with increasing I_L characterize the inhibition type. Thus, the plot of $k_{\max}^{app}$ vs. K_s^{app} (i.e., a direct linear plot) is very useful in identifying the inhibition type, because it visualizes the parameter variation patterns (Cornish-Bowden, 1994).

Direct Linear Plot

The direct linear plot of Eisenthal and Cornish-Bowden (1974) and Cornish-Bowden and Eisenthal (1978) was

Table I. The effects of inhibitors on the parameters of the Michaelis-Menten equation and linearized inhibition equations.

Type of inhibition	$k_{\max}^{app}$ $0 < I_L < \infty$	$k_{\max}^{app}$ $I_L \to \infty$	K_s^{app} $0 < I_L < \infty$	K_s^{app} $I_L \to \infty$	Linearized inhibition equation ($0 < I_L < \infty$)
Mixed (Mix)	$\frac{k_{max}}{(1+\frac{I_L}{K_{iu}})}$	0	$\frac{K_s(1+\frac{I_L}{K_{ic}})}{(1+\frac{I_L}{K_{iu}})}$	$\frac{K_{iu}K_s}{K_{ic}}$	$\frac{K_s^{app}}{k_{\max}^{app}} = \frac{K_s}{k_{max}} + \frac{K_s}{k_{max}K_{ic}} I_L$ $\frac{1}{k_{\max}^{app}} = \frac{1}{k_{max}} + \frac{1}{k_{max}K_{iu}} I_L$
Noncompetitive (NC)	$\frac{k_{max}}{(1+\frac{I_L}{K_{iu}})}$	0	K_s	K_s	$\frac{1}{k_{\max}^{app}} = \frac{1}{k_{max}} + \frac{1}{k_{max}K_{iu}} I_L$ $K_s = K_s^{app}$
Competitive (Com)	k_{max}	k_{max}	$K_s(1+\frac{I_L}{K_{ic}})$	∞	$K_s^{app} = K_s + \frac{K_s}{K_{ic}} I_L$ $k_{max} = k_{\max}^{app}$
Uncompetitive (UC)	$\frac{k_{max}}{(1+\frac{I_L}{K_{iu}})}$	0	$\frac{K_s}{(1+\frac{I_L}{K_{iu}})}$	0	$\frac{1}{K_s^{app}} = \frac{1}{K_s} + \frac{1}{K_s K_{iu}} I_L$ $\frac{1}{k_{\max}^{app}} = \frac{1}{k_{max}} + \frac{1}{k_{max}K_{iu}} I_L$

Note: I_L = inhibitor concentration in liquid phase (μM); K_{ic} = competitive inhibition coefficient (μM); K_{iu} = uncompetitive inhibition coefficient (μM). Adapted from Cornish-Bowden, 1994.

used to determine the inhibition types. Eq. (1) can be rearranged to show the dependence of k_{max}^{app} on K_s^{app}:

$$k_{max}^{app} = v + \frac{v}{S_L} K_s^{app} \quad (5)$$

If k_{max}^{app} and K_s^{app} are treated as variables, and v and S_L as constants, this equation defines a straight line of slope v/S_L, y-axis intercept v and x-axis intercept $-S_L$. The straight line drawn according to Eq. (5) relates all pairs of k_{max}^{app} and K_s^{app} values that satisfy one observation exactly. A second line drawn for a second observation will relate all pairs of k_{max}^{app} and K_s^{app} values that satisfy the second observation exactly. An intersection point of the two lines defines the unique pair of k_{max}^{app} and K_s^{app} values that satisfy both observations exactly. Ideally, there should be one intersection point that satisfies several observations. However, several intersection points are typically obtained from the plot. The medians of each set of k_{max}^{app} and K_s^{app} (rather than averages) provide best estimates. Although the median values can be obtained from graphic analyses, external calculation using each set of k_{max}^{app} and K_s^{app} was performed to provide more accurate values.

An example of a direct linear plot in the case of 1,1,1-TCA transformation in the absence of butane is shown in Figure 2A. Values of v are plotted on the vertical axis and the corresponding negative S_L values are plotted on the horizontal axis. The corresponding points are then joined and extrapolated, with intersections (small open circle) defining a unique pair of k_{max}^{app} and K_s^{app} values

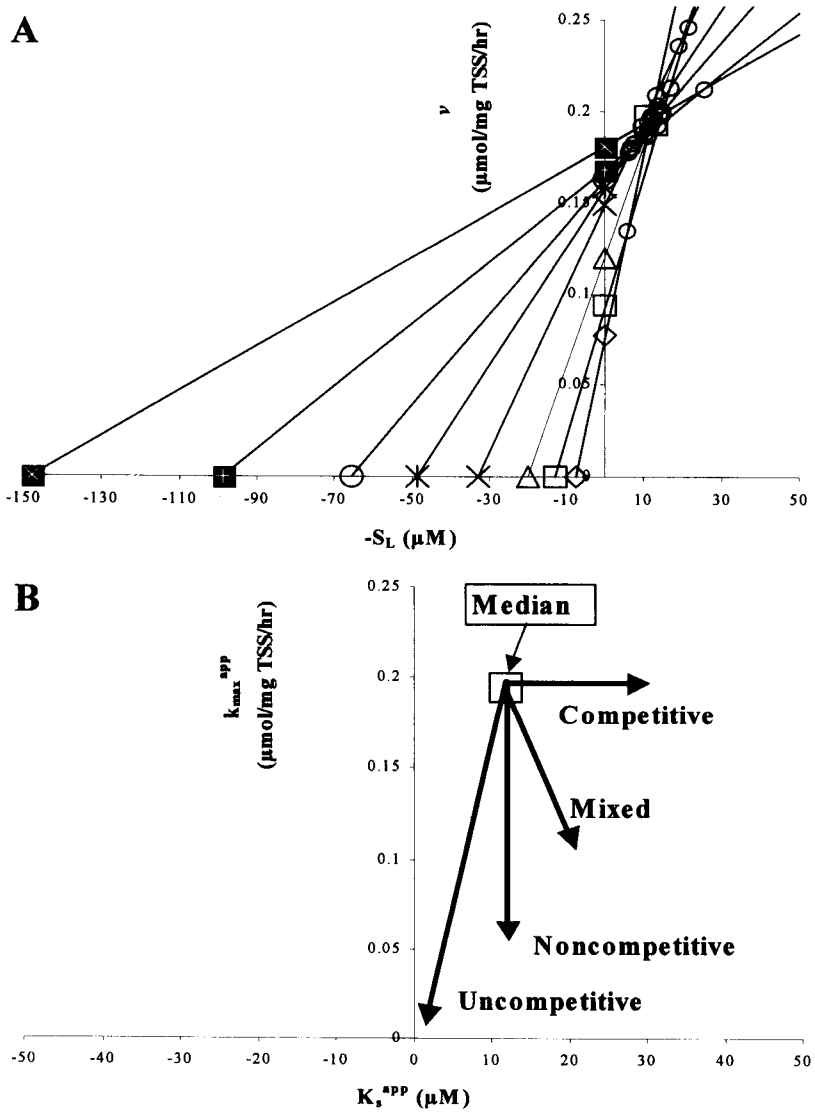

Figure 2. Direct linear plot of v against $-S_L$ in the case of 1,1,1-TCA transformation in the absence of butane (A) and a plot of k_{max}^{app} against K_s^{app} (B). In panel A the symbols on the vertical axis represent v values, and the same symbols on the horizontal axis represent the corresponding negative S_L values. A small open circle at an intersection of two lines represents a unique pair of k_{max}^{app} and K_s^{app} values that satisfy two sets of observations, and a large open square symbol represents the best estimates of k_{max}^{app} and K_s^{app}.

that satisfy two sets of observations. The medians of each set of k_{max}^{app} and K_s^{app} provide best estimates (large open square symbol). As shown in Figure 2A, the k_{max} and K_s for 1,1,1-TCA are 0.20 μmol/mg TSS/h and 12 μ*M*, respectively.

As discussed above, the variation patterns of both k_{max}^{app} and K_s^{app} (with increasing I_L) can be used to identify the inhibition type. Direct linear plots with only the best estimate (median) point (k_{max}^{app}, K_s^{app}) plotted at various levels of I_L result in shifting directions of the best estimate point (k_{max}^{app}, K_s^{app}) (Fig. 2B). Note that axis titles in Figure 2B are different from those in Figure 2A, because only best estimate values for k_{max}^{app} and K_s^{app} are plotted in Figure 2B. By definition, for competitive inhibition, the shift is to the right; for uncompetitive inhibition, it is directly toward the origin; for mixed inhibition, it is intermediate between these extremes; and for noncompetitive inhibition (a special case of mixed inhibition), it shifts down vertically (Cornish-Bowden, 1994).

Determination of k_{max}, K_s, K_{ic}, and K_{iu}

For single compound batch kinetic studies, k_{max} and K_s were determined by fitting the kinetic data to Eq. (3) using NLSR in S-PLUS (MathSoft Inc., Cambridge, MA). To estimate the k_{max} and K_s values by the NLSR routine, degradation/transformation rates along with corresponding substrate and inhibitor concentrations were given as an input data, and Eq. (3) was used to obtain a best fit to the data. Initial estimates (guesses) of k_{max} and K_s for NLSR routine were obtained by Monod plots of rate vs. substrate concentration.

In the inhibition studies, k_{max}, K_s, K_{ic}, and K_{iu} were determined by NLSR analysis for the inhibition model determined by the direct linear plot method. Linear regression of the linearized forms presented in Table I was used to obtain the initial guesses of all kinetic parameters for the NLSR fitting. The derivations of the linearized forms in Table I are presented by Kim (2000). Mixed inhibition is a more complex kinetic expression with more parameters compared to the other kinetic equations. The linearized forms provided good initial parameter guesses that are needed for the NLSR method to converge, especially for the case of mixed inhibition.

Method Used in This Study

A combined method for determining kinetic parameters, inhibition type, and inhibition coefficients of aerobic CAH transformation is presented in this study. Plots of k_{max}^{app} vs. K_s^{app} (derived from direct linear plots) at various levels of I_L (Fig. 2B) were used to visually identify the inhibition type (Cornish-Bowden, 1994). After identifying the inhibition type, the appropriate linearized equations in Table I were used to obtain initial guesses of kinetic parameters for NLSR analysis. The k_{max}^{app} and K_s^{app} values obtained from direct linear plots were used as data inputs for regression of the linearized equations for all inhibition cases. In the case of mixed inhibition, $1/k_{max}^{app}$ was plotted against I_L. The slope and y intercept represents $1/(k_{max}K_{iu})$ and $1/k_{max}$, respectively. From these values, k_{max} and K_{iu} were calculated. The values for K_s and K_{ic} were obtained from a second plot of K_s^{app}/k_{max}^{app} vs. I_L. Thus, for the mixed inhibition case all the parameters were obtained from these two linearized plots. In the case of competitive inhibition, K_s^{app} was plotted against I_L. The slope and intercept represent K_s/K_{ic} and K_s, respectively. From these values, K_s and K_{ic} were calculated. The k_{max} was calculated by averaging the values of k_{max}^{app} obtained from direct linear plot. The same procedures can be applied to the other inhibition cases to obtain kinetic parameters.

RESULTS

Acetylene Blocking Experiment

Results of the acetylene inactivation experiment performed to evaluate the kinetic diversity of butane-oxidizers in the mixed culture are presented in Figure 3. A progressive loss of butane uptake rate as a function of time was observed. The natural log of residual butane uptake activity [rate at time t (r) to rate at time zero (r_0)] is plotted as a function of time. The results fit a first-order kinetics inactivation model well ($R^2 = 0.96$), and were consistent with observations of Keener et al. (1998)

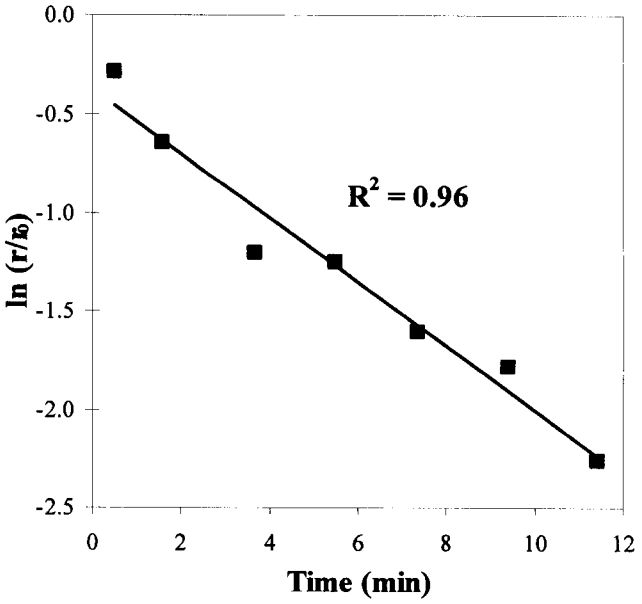

Figure 3. Loss of butane degradation rate as a function of time after acetylene exposure. Data were fit to first order decay model. The ratio of the rate at time t to that at time zero is represented by r/r_0.

with nitrifying bacteria. This fit to a first-order kinetics inactivation model indicates that kinetically similar monooxygenases are present in a butane-grown mixed culture. Thus, applying the inhibition kinetics developed for homogenous enzyme systems was a reasonable assumption.

k_{max} and K_s for Butane and 1,1,1-TCA

k_{max} and K_s for butane and 1,1,1-TCA were determined in single compound tests with the butane-grown mixed culture. In butane batch kinetic tests, the amount of cell mass increase resulting from butane degradation was less than 5% of initial cell mass added. Thus, cell growth had little effect on initial rate of butane degradation. The measured degradation rates of butane (A) and transformation rates of 1,1,1-TCA (B) vs. concentration are provided in Figure 4, along with the best-fit curves to Eq. (3) achieved by NLSR. Excellent agreement to the equation was achieved. The estimated k_{max} and the 95% confidence intervals for butane and 1,1,1-TCA were 2.6 ± 0.14 and 0.19 ± 0.01 μmol/mg TSS/h, respectively, whereas the K_s values were 19 ± 3.3 and 12 ± 2.8 μ*M*, respectively (Table II). For 1,1,1-TCA, k_{max} and K_s were in excellent agreement with those determined from the direct linear plot (Fig. 2A). Although the K_s values for butane and 1,1,1-TCA are in a similar range, the k_{max} for butane degradation is over an order of magnitude greater than the k_{max} for 1,1,1-TCA transformation.

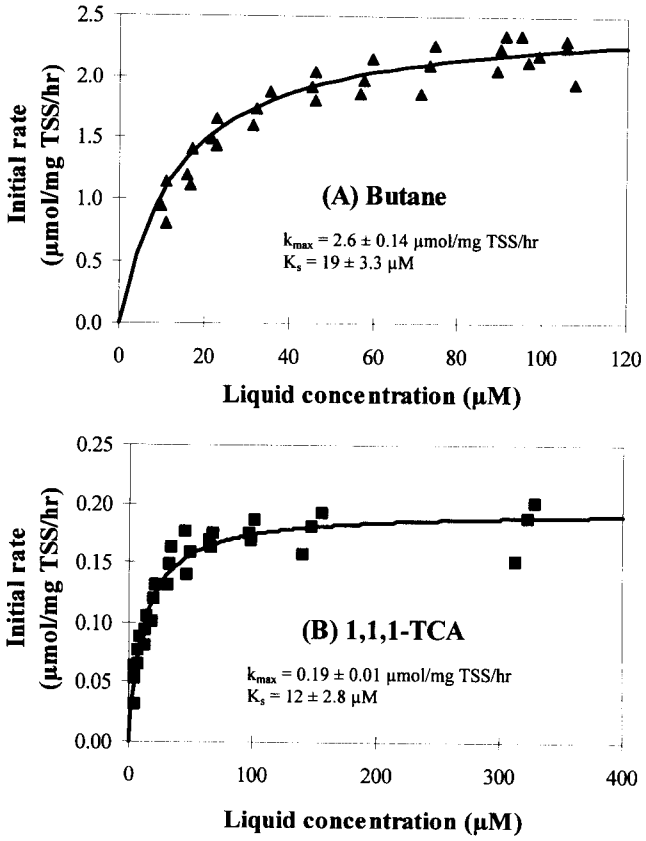

Figure 4. Initial degradation rates at various initial concentrations of butane (A) and 1,1,1-TCA (B). The curve represents the best fit of data to Eq. (3) using NLSR.

Inhibition Types and Inhibition Coefficients

1,1,1-TCA Inhibition on Butane Degradation

The inhibition of butane degradation by 1,1,1-TCA was first investigated by measuring initial butane degradation rates at four butane concentrations (3.2, 12, 23, 40 μ*M*) and five different inhibitor (1,1,1-TCA) concentrations (0, 184, 548, 902, 1228 μ*M*). Butane concentrations were chosen to include values ranging from 0.2 to 2.0 the K_s for butane. The direct linear plot showing inhibition of 1,1,1-TCA on butane degradation is presented in Figure 5A. The points of intersection, shown as smaller symbols, give the estimate of k_{max}^{app} and K_s^{app}. The best estimate of k_{max}^{app} and K_s^{app}, shown as the larger symbols, are the medians of the individual values at the various I_L concentrations (1,1,1-TCA). As the inhibitor concentration increases, the K_s^{app} for butane also increases, whereas k_{max}^{app} for butane remains essentially constant, indicating competitive inhibition of 1,1,1-TCA on butane degradation.

Kinetic parameters (K_{ic} and K_s) were graphically estimated by the plot of K_s^{app} vs. I_L (Fig. 5B). For the competitive inhibition model the plot of these variables

Table II. Comparison of k_{max}, K_s, K_{ic}, and K_{iu} that are separately estimated from single-compound rate studies, and linear plots and NLSR analysis using rate data in the presence of inhibitors.

Method	Butane		1,1,1-TCA		Inhibitor and inhibition coefficients		
	k_{max} (μmol/ mg TSS/h)	K_s (μ*M*)	k_{max} (μmol/ mg TSS/h)	K_s (μ*M*)	Butane K_{ic} (μ*M*)	Butane K_{iu} (μ*M*)	1,1,1-TCA K_{ic} (μ*M*)
Single compound test	2.6 ± 0.14[a]	19 ± 3.3	0.19 ± 0.01	12 ± 2.8	–	–	–
Linearized equation	2.4	12	0.23	18	0.52	0.36	350
NLSR	2.5 ± 0.31	13 + 4.4	0.20 ± 0.007	19 ± 2.1	0.28 ± 0.1	0.51 ± 0.1	313 ± 88

[a]The errors represent 95% confidence intervals.

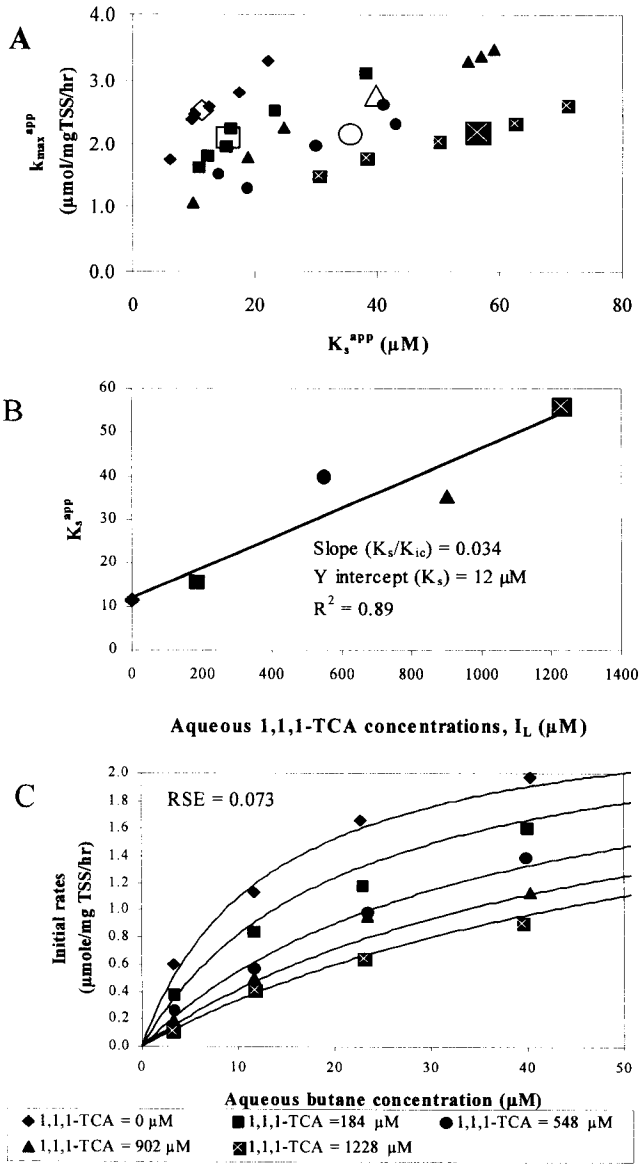

Figure 5. Direct linear plot showing competitive inhibition of 1,1,1-TCA on butane degradation (A), plot of K_s^{app} versus I_L to graphically evaluate K_s and K_{ic} (B), and the NLSR best fit of the data to the competitive inhibition equation (C). In panel A the points of intersection, shown as smaller symbols, give the estimate of k_{max}^{app} and K_s^{app} and the best estimate of k_{max}^{app} and K_s^{app}, shown as the larger symbols, are the medians of the individual values at the various I_L concentrations (1,1,1-TCA).

yields a linear correlation with K_s/K_{ic} equal to the slope and K_s equal to y intercept (Table I). As shown in Figure 5B, a linear plot was achieved with an R^2 value of 0.89. Linear regression yielded a K_s value of 12 μ*M* for butane and a K_{ic} value of 350 μ*M* for 1,1,1-TCA. The K_s value for butane is close to the value (19 μ*M*) determined from the single compound test (Table II). The k_{max} value of butane (2.4 μmol/mg TSS/h) calculated by averaging the k_{max}^{app} values obtained from the direct linear plot was also within the range of the value (2.6 μmol/mg TSS/h) determined in the single compound test.

The linear regression values of k_{max}, K_s, and K_{ic} (Fig. 5B) were used as initial guesses for the NLSR fitting analysis. The data converged with very small residual standard error (RSE) of 0.073 (Fig. 5C), yielding a K_{ic} value of 313 ± 88 μ*M* for 1,1,1-TCA, which was in the range of the linearized K_{ic} value of 350 μ*M* used as the initial guess. k_{max} and K_s for butane were 2.5 ± 0.31 μmol/mg TSS/h and 13 ± 4.4 μ*M*, respectively, in good agreement with the values from the single compound tests.

Butane Inhibition of 1,1,1-TCA Transformation

Inhibition of butane on 1,1,1-TCA transformation was also evaluated. As shown in Figure 6A, the shift pattern of k_{max}^{app} and K_s^{app} with increasing inhibitor (butane) concentration can be interpreted as mixed, uncompetitive, or noncompetitive inhibition. Uncompetitive inhibition is not an appropriate model in this case, because an uncompetitive inhibitor only binds to ES (enzyme substrate complex). That is, it only binds and degrades in the presence of substrate. However, butane degrades in the absence of 1,1,1-TCA, so butane is not an uncompetitive inhibitor on 1,1,1-TCA transformation. Mixed inhibition is more inclusive than noncompetitive inhibition; thus, we interpret it as mixed inhibition of butane on 1,1,1-TCA transformation. The kinetic parameters (k_{max}, K_s, K_{iu}, and K_{ic}) were estimated by linear regression of the equations in Table I for the mixed inhibition case (Fig. 6B). Excellent fits to the linearized forms were obtained. The k_{max} and K_s values for 1,1,1-TCA were 0.23 μmol/mg TSS/h and 18 μ*M*, respectively, which agreed well with the values obtained in the single compound tests. The K_{iu} and K_{ic} for butane were 0.52 μ*M* and 0.36 μ*M*, respectively. NLSR analysis (shown in Fig. 6C) yielded an excellent agreement to the mixed inhibition model. Both inhibition coefficients (K_{iu} = 0.51 ± 0.1 μ*M* and K_{ic} = 0.28 ± 0.1 μ*M*) were similar to the values obtained from the linear plot and used as initial guesses for NLSR (Table II).

Comparison of Kinetic Parameters Determined with Different Methods

Table II summarizes k_{max} and K_s values determined from single compound tests and from inhibition tests using linearized equation plots and NLSR analysis. The K_s of butane determined by both the linear plots and NLSR analyses are slightly lower than the values obtained from the single compound tests. All methods yielded very comparable K_s values for 1,1,1-TCA. The k_{max} values determined by all three methods are in excellent agreement. The results suggest that k_{max} and K_s values can be very effectively determined from inhibition test results by either the linear plot method, or NLSR

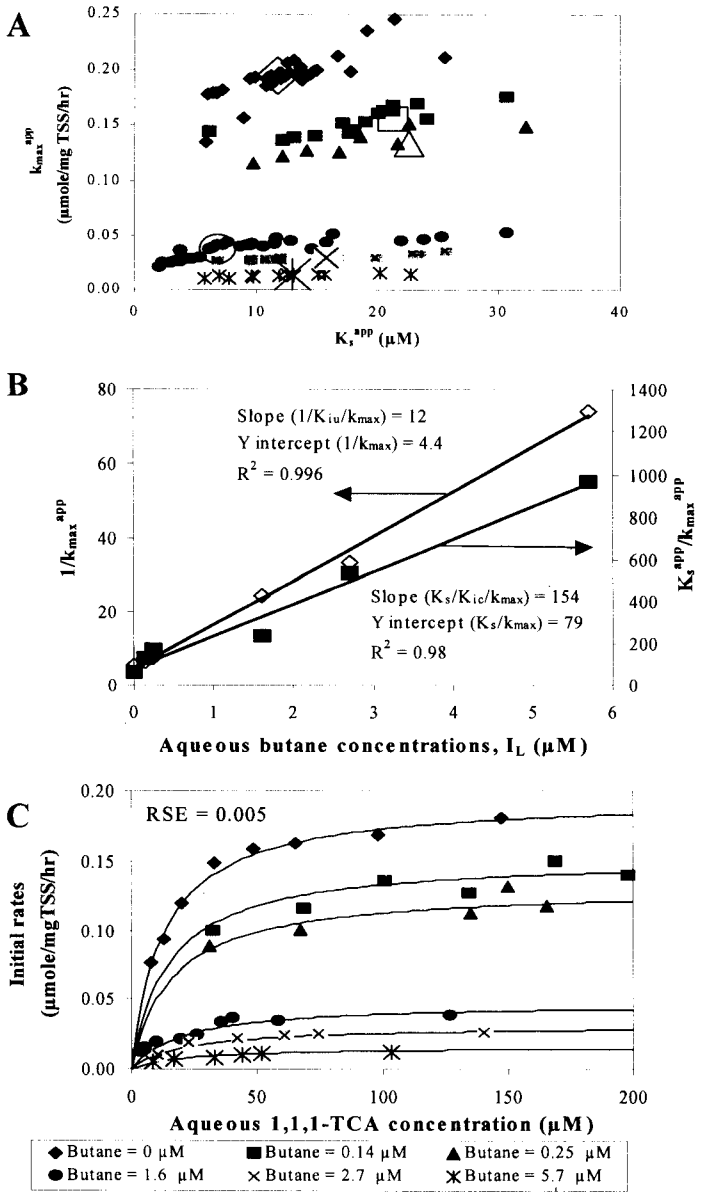

Figure 6. Direct linear plot showing mixed inhibition of butane on 1,1,1-TCA transformation (A), plot of $1/k_{max}^{app}$ or K_s^{app}/k_{max}^{app} versus I_L to graphically evaluate k_{max}, K_s, K_{ic}, and K_{iu} (B) and the NLSR best fit of the data to the mixed inhibition equation (C). In panel A the points of intersection, shown as smaller symbols, give the estimate of k_{max}^{app} and K_s^{app}, and the best estimate of k_{max}^{app} and K_s^{app} shown as the larger symbols, are the medians of the individual values at the various I_L concentrations (butane).

analysis using initial guesses obtained from the linear plot.

Effects of k_{max} and/or K_s on Inhibition Coefficients in NLSR Analysis

In the previous NLSR analyses all kinetic parameters in the inhibition equations were permitted to vary in obtaining the model fit to the experimental data. To evaluate how k_{max} and/or K_s affect the determination of inhibition coefficients (K_{ic} and K_{iu}) during NLSR analysis, k_{max} and/or K_s obtained from the single compound tests were provided as constants for the NLSR analysis. Four different NLSR analyses were performed: (1) varying all kinetic parameters (k_{max}, K_s, K_{ic}, and/or K_{iu}); (2) constant k_{max} and K_s and varying inhibition coefficients; (3) constant k_{max} and varying K_s and inhibition coefficients; and (4) constant K_s and varying k_{max} and inhibition coefficients.

Table III presents the inhibition coefficients (K_{ic} and/or K_{iu}), determined with the four different NLSR analyses using initial guesses of the inhibition parameters from the linearized plot. For both inhibition cases, the NLSR analyses yielded estimated inhibition coefficients the 95% confidence intervals of which overlapped each other. The results suggest that prior determination of k_{max} and/or K_s in single compound tests is not required

Table III. Comparison of K_{ic} and K_{iu} obtained with different methods.

	Inhibitor[a]		
	Butane	Butane	1,1,1-TCA
Method	K_{ic} (μM)	K_{iu} (μM)	K_{ic} (μM)
NLSR[b]	0.28 ± 0.1	0.51 ± 0.1	313 ± 88
NLSR $k_{max}K_s$[c]	0.25 ± 0.1	0.56 ± 0.1	419 ± 65
NLSR k_{max}[d]	0.24 ± 0.1	0.56 ± 0.1	318 ± 72
NLSR K_s[e]	0.25 ± 0.1	0.53 ± 0.1	356 ± 64

[a]Kinetic parameter are presented with 95% confidence interval.
[b]NLSR with all kinetic parameters varying (k_{max}, K_s, K_{ic}, and/or K_{iu}).
[c]NLSR with constant k_{max} and K_s and with two inhibition coefficients varying.
[d]NLSR with constant k_{max} and with K_s and two inhibition coefficients varying.
[e]NLSR with constant K_s, and with k_{max} and two inhibition coefficients varying.

for determining the inhibition coefficients (K_{ic} and K_{iu}). The good agreement of k_{max} and K_s values obtained using different methods, shown in Table II, indicate that this would be the likely result of this analysis.

NLSR Analysis with Different Inhibition Models

To evaluate how the data fit to different inhibition models and how the models affect the estimated kinetic parameters, NLSR analysis using three different inhibition model equations was performed with the inhibition data. For this comparison all kinetic parameters were varied and minimized in the NLSR analysis. This analysis evaluated how the data best fit by a mixed inhibition model would be fit using a competitive inhibition model and vice versa, or how data best fit by a mixed inhibition model fit a noncompetitive inhibition model.

The mixed inhibition and the noncompetitive inhibition model NLSR fits to the data showing competitive inhibition of 1,1,1-TCA on butane degradation (Fig. 5A) are tested, and Table IV summarizes the kinetic and inhibition parameters in this fitting exercise. The inhibition data was also well fit by mixed and noncompetitive inhibition models, having the comparable RSE as competitive inhibition fit. For butane, the k_{max} and K_s values were in the range determined using the competitive inhibition model. This result illustrates the importance of using the direct linear plot to identify the inhibition type, since NLSR does not clearly distinguish between inhibition types based on the RSE values. For the case of mixed inhibition model, K_{ic} was in the range determined using the competitive inhibition model. However, the estimated K_{iu} value was a factor of 26 times greater than K_{ic}, and K_{iu} value had much greater error than the K_{ic} estimate. Data showing competitive inhibition is represented by a mixed inhibition model having a very high K_{iu} to compensate for the inhibitor effect on K_{max}.

To noncompetitive inhibition and competitive inhibition models. Data showing mixed inhibition of butane on 1,1,1-TCA transformation (Fig. 6A) were fit by NLSR. The data could also be well fit to the noncompetitive inhibition model, having the same RSE as mixed inhibition fit. Data when fit to the competitive inhibition model resulted in a higher RSE than those achieved with the mixed and noncompetitive inhibition models. The k_{max}, K_s, and/or K_{iu} obtained from noncompetitive and competitive inhibition model fits were in the range of the values determined from the fit to the mixed inhibition model (Table II). The reason for the good fit of the noncompetitive inhibition model is that K_{ic} and K_{iu} for butane were very close, thus K_s^{app} is equal to K_s resulting in noncompetitive inhibition model as shown in Table I. This result is consistent with the near vertical shift in k_{max}^{app} shown Figure 6A, indicating that it is difficult to distinguish between mixed and noncompetitive inhibition for this case.

DISCUSSION

A systematic kinetic and inhibition study of aerobic cometabolism of 1,1,1-TCA, by a butane-grown mixed culture is presented. The method that combined both direct linear plots to identify the inhibition type and NLSR analysis to estimate the kinetic parameters, using

Table IV. Kinetic parameters (k_{max} and K_s) for a substrate and inhibition coefficients for an inhibitor obtained from NLSR analysis by fitting different inhibition models to the data.

Substrate	Inhibitor	Inhibition type	k_{max} (μmol/mgTSS/hr)	K_s (μM)	K_{ic} (μM)	K_{iu} (μM)	Residual standard error
Butane	1,1,1-TCA	Com[a]	2.53 ± 0.31	13.1 ± 4.4	313 ± 88	–	0.073
		Mix	2.6 ± 0.38	13.6 ± 5.3	346 ± 189	8915 ± 42184	0.075
		NC	3.1 ± 0.53	21.6 ± 7.7	–	964 ± 215	0.093
1,1,1-TCA	Butane	Mix[a]	0.20 ± 0.01	12.7 ± 2.1	0.28 ± 0.1	0.51 ± 0.1	0.005
		NC	0.20 ± 0.01	19.1 ± 4.3	–	0.50 ± 0.08	0.005
		Com	0.18 ± 0.01	9.4 ± 3.3	0.05 ± 0.02	–	0.011

[a]Inhibition type determined by the direct linear plot.

graphically estimated kinetic parameters as initial guesses, proved to be very effective. The inhibition of butane degradation by 1,1,1-TCA demonstrates the usefulness of this combined approach. The data are consistent with competitive inhibition and all three methods (single compound test, linear plot, and NLSR analysis) gave similar values of k_{max} and K_s. However, the data also reveal the importance of combining a graphical representation of the data with a NLSR analysis when determining the inhibition type. Note that good fits (based on RSE) were obtained with all three models (Table IV).

NLSR analysis requires initial guesses of the parameters, which, if good, will result in a convergence to best-fit estimates at a global minimum of RSE instead of a local minimum. The linearized equations presented in Table I are useful in providing these guesses. Shown in Table II are the comparison of values obtained from the linearized equations, single compound kinetic tests, and the final values obtained by NLSR. Most of the estimates obtained from the linearized method and single compound kinetic tests for k_{max} and K_s are in the range achieved by NLSR, indicating convergence to best-fit estimates at a global minimum of RSE. The direct linear plots also provide visual insight into the inhibition type and initial guesses needed for linear and NLSR estimates. For most cases this approach resulted in a distribution of data that was amendable to linear regression of the equations in Table I.

Our kinetic results with a butane-grown mixed culture can be compared to other cometabolic systems. Kinetic parameters for 1,1,1-TCA were determined with *M. trichosporium* OB3b producing soluble methane monooxygenase (sMMO) (Oldenhuis et al., 1991) and with a mutant methanotroph *M. trichosporium* OB3b PP358 constitutively expressing sMMO (Aziz et al., 1999). The K_s for 1,1,1-TCA measured here was a factor of 20 lower than the value Oldenhuis et al. (1991) reported, whereas k_{max} was an order of magnitude lower. Little transformation of 1,1,1-TCA and very low affinity of sMMO for 1,1,1-TCA was reported with *M. trichosporium* OB3b PP358. Thus, this comparison suggests that the butane-grown culture also has higher affinity for 1,1,1-TCA, but potentially slower maximum transformation rates.

With respect to in situ cometabolic treatment of CAHs, the contaminant concentrations are often much lower than the K_s. Thus, the pseudo first-order rate ($k_1 = k_{max}/K_s$) is a more important parameter. The k_1 for 1,1,1-TCA obtained with our enrichment is comparable to that with *M. trichosporium* OB3b (Oldenhuis et al., 1991), and it is much higher than that with mutant methanotroph *M. trichosporium* OB3b PP358 constitutively expressing sMMO (Aziz et al., 1999). The k_1 values obtained with methane- or propane-grown mixed cultures studied by Strand et al. (1990) and Keenan et al. (1994) are 2 to 4 orders of magnitude lower than observed here. Thus, the butane-grown culture studied here has potential advantages for bioremediation of 1,1,1-TCA.

Inhibition of CAHs on growth substrate utilization or vice versa is an important consideration in the design of effective systems for cometabolizing CAHs, because it is strongly related to microorganism growth and/or viability and enzyme activity (Alvarez-Cohen and McCarty, 1991; Anderson and McCarty, 1996; van Hylckama Vlieg et al., 1997). Most modeling of inhibition of CAH cometabolism has assumed or found competitive inhibition kinetics (Anderson and McCarty, 1996; Chang and Alvarez-Cohen, 1995, 1996; Chang and Criddle, 1997; Semprini, 1995). However, there are reports that other inhibition models may apply. For example, the inhibitory effect of 1,1,1-TCA on methane consumption (Broholm et al., 1992) and propane on 1,1,1-TCA transformation (Keenan et al., 1994) did not fit a competitive inhibition model. Also, in a study with *N. europaea,* the ability of several alternative substrates to inhibit AMO oxidation of NH_3 was tested (Keener and Arp, 1993). Some nonhalogenated C1 and C2 compounds, such as ethylene and methane, were competitive inhibitors of NH_3 oxidation. Larger nonhalogenated compounds such as propane, butane, and monohalogenated compounds such as chloromethane and chloroethane noncompetitively (in this study, defined as mixed inhibition) inhibited NH_3 oxidation. In results presented here, competitive inhibition of 1,1,1-TCA on butane degradation was observed. However, butane showed mixed inhibition on 1,1,1-TCA transformation. Thus, competitive inhibition and mixed inhibition are both important in the cometabolism of CAHs. The types of inhibition mechanisms observed may differ with different microorganisms, growth substrates, and CAHs.

The butane-degradation dependent inactivation of cells by acetylene was well fit by a first-order-decay model. These results suggest that a kinetically similar population of butane-oxidizers was responsible for the degradation of butane and 1,1,1-TCA. Thus, mixed inhibition of butane on CAHs transformation does not likely result from the kinetic diversity of mixed culture. Other mechanisms cannot be ruled out, because the measurements were done with whole cells and not with purified enzymes. Thus, substrate transport to the enzyme and other cell dynamic processes may have an influence on the inhibition observed. Detailed studies with pure cultures and with purified enzymes are needed to further demonstrate the utility of this method.

This article has not been reviewed by the U.S. Environmental Protection Agency, and no official endorsement should be inferred. We acknowledge the help of Dr. James M. Tiedje for discussions on the interpretation of these data. We also thank Adisorn Tovanabootr, Dr. Mark Dolan, George Pon, and Incheol Pang for helping to measure overall mass transfer coefficients.

NOMENCLATURE

H_{cs}	dimensionless Henry's constant of substrate (–)
H_{ci}	dimensionless Henry's constant of inhibitor (–)
I_L	inhibitor concentrations in liquid phase (μM)
k_{max}^{app}	apparent maximum degradation/transformation rates (μmol/mg TSS/h)
K_s^{app}	apparent half-saturation coefficient (μM)
K_{ic}	competitive inhibition coefficient (μM)
K_{iu}	uncompetitive inhibition coefficient (μM)
k_{max}	maximum degradation/transformation rates (μmol substrate/mg TSS/h)
K_s	half-saturation coefficient (μM)
M_i	total inhibitor mass (μmol)
M_s	total substrate mass (μmol)
S_L	substrate concentrations in liquid phase (μM)
t	time (minutes or hour)
v	specific substrate degradation rates (μmol/mg TSS/h)
V_L	volume of liquid phase (L)
V_G	volume of gas phase (L)

References

Alvarez-Cohen L, McCarty PL. 1991. Product toxicity and cometabolic competitive inhibition modeling of chloroform and trichloroethylene transformation by methanotrophic resting cells. Appl Environ Microbiol 57:1031–1037.

American Public Health Association. 1985. Standard methods for the examination of water and wastewater, 16th ed. New York: APHA.

Anderson JE, McCarty PL. 1994. Model for treatment of trichloroethylene by methanotrophic biofilms. J Environ Eng 120:379–400.

Anderson JE, McCarty PL. 1996. Effect of three chlorinated ethenes on growth rates for a methanotrophic mixed culture. Environ Sci Technol 30:3517–3524.

Anderson JE, McCarty PL. 1997. Transformation yield of chlorinated ethenes by a methanotrophic mixed culture expressing particulate methane monooxygenase. Appl Environ Microbiol 63:687–693.

Aziz CE, Georgiou GE, Speitel Jr. GE. 1999. Cometabolism of chlorinated solvents and binary chlorinated solvent mixtures using *M. trichosporium* OB3b PP358. Biotechnol Bioeng 65:100–107.

Broholm K, Christensen TH, Jensen BK. 1992. Modeling TCE degradation by a mixed culture of methane-oxidizing bacteria. Water Res 9:1177–1185.

Chang HL, Alvarez-Cohen L. 1995. Transformation capacities of chlorinated organics by mixed cultures enriched on methane, propane, toluene or phenol. Biotechnol Bioeng 45:440–449.

Chang HL, Alvarez-Cohen L. 1996. Biodegradation of individual and multiple chlorinated aliphatic hydrocarbons by methane-oxidizing cultures. Appl Environ Microbiol 62:3371–3377.

Chang HL, Alvarez-Cohen L. 1997. Two-stage methanotrophic bioreactor for the treatment of chlorinated organic wastewater. Water Res 31:2026–2036.

Chang W-K, Criddle CS. 1997. Experimental evaluation of a model for cometabolism: prediction of simultaneous degradation of trichloroethylene and methane by a methanotrophic mixed culture. Biotechnol Bioeng 54:491–501.

Cornish-Bowden A. 1994. Fundamentals of enzyme kinetics. London; Portland Press.

Cornish-Bowden A, Eisenthal R. 1978. Estimation of Michaelis constant and maximum velocity from the direct linear plot. Biochim Biophys Acta 523:268–272.

Dowd JE, Riggs DS. 1965. A comparison of estimates of Michaelis-Menten kinetic constants from various linear transformations. J Biol Chem 240:863–869.

Eisenthal R, Cornish-Bowden A. 1974. The direct linear plot: a new graphical procedure for estimating enzyme kinetic parameters. Biochem J 139:715–720.

Ely RL, Williamson KJ, Hyman MR, Arp DJ. 1997. Cometabolism of chlorinated solvents by nitrifying bacteria: kinetics, substrate interaction, toxicity effects, and bacterial response. Biotechnol Bioeng 54:520–534.

Gossett JM. 1987. Measurements of Henry's law constants for C1 and C2 chlorinated hydrocarbons. Environ Sci Technol 21:202–208.

Hamamura N, Storfa RT, Semprini L, Arp DJ. 1999. Diversity in butane monooxygenase among butane-grown bacteria. Appl Environ Microbiol 65:4586–4593.

Hopkins GD, McCarty PL. 1995. Field observations of in situ aerobic cometabolism of trichloroethylene and three dichloroethylene isomers using phenol and toluene as primary substrates. Environ Sci Technol 29:1628–1637.

Hopkins GD, Semprini L, McCarty PL. 1993. Microcosm and in situ field studies of enhanced biotransformation of trichloroethylene by phenol-utilizing microorganisms. Appl Environ Microbiol 59:2277–2285.

Keenan JE, Strand SE, Stensel HD. 1994. Degradation kinetics of chlorinated solvents by a propane-oxidizing enrichment culture. In: Hinchee RE, Leeson A, Semprini L, Ong SK, editors. Bioremediation of chlorinated and polycyclic aromatic hydrocarbon compounds. Boca Raton, FL; Lewis Publishers. p 1–13.

Keener WK, Arp DJ. 1993. Kinetic studies of ammonia monooxygenase inhibition in *Nitrosomonas europaea* by hydrocarbons and halogenated hydrocarbons in an optimized whole-cell assay. Appl Environ Microbiol 59:2501–2510.

Keener WK, Russell SA, Arp DJ. 1998. Kinetic characterization of the inactivation of ammonia monooxygenase in *Nitrosomonas europaea* by alkyne, aniline, and cyclopropane derivatives. Biochim Biophys Acta 1388:373–385.

Kim Y. 2000. Aerobic cometabolism of chlorinated aliphatic hydrocarbons by a butane-grown mixed culture: transformation abilities, kinetics and inhibition. PhD dissertation. Oregon State University, Corvallis, OR.

Kim Y, Arp DJ, Semprini L. 2000. Aerobic cometabolism of chlorinated methanes, ethanes, and ethenes, by a butane-grown mixed culture. J Environ Eng 126:934–942.

Kim Y, Semprini L, Arp DJ. 1997. Aerobic cometabolism of chloroform and 1,1,1-trichloroethane by butane-grown microorganisms. Bioremed J 2:135–148.

Landa AS, Sipkema EM, Weijma J, Beenackers AACM, Dolfing J, Janssen DB. 1994. Cometabolic degradation of trichloroethylene by *Pseudomonas cepacia* G4 in a chemostat with toluene as the primary substrate. Appl Environ Microbiol 60:3368–3374.

Mackay D, Shiu WY. 1981. A critical review of Henry's law constants for chemicals of environmental interest. J Phys Chem Ref Data 10:1175–1199.

Oldenhuis R, Oedzes JY, van der Waarde JJ, Janssen DB. 1991. Kinetic of chlorinated hydrocarbon degradation by *Methylosinus trichosporium* OB3b and toxicity of trichloroethylene. Appl Environ Microbiol 57:7–14.

Prior SD, Dalton H. 1985. Acetylene as a suicide substrate and active site probe for methane monooxygenase from *Methylococcus capsulatus* (Bath). FEMS Microbiol Lett 29:105–109.

Robinson JA. 1985. Determining microbial kinetic parameters using nonlinear regression analysis. Adv Microb Ecol 8:61–114.

Robinson JA, Charaklis WG. 1984. Simultaneous estimation of V_{max}, K_m, and the rate of endogenous substrate production (R) from substrate depletion data. Microb Ecol 10:165–178.

Semprini L. 1995. In situ bioremediation of chlorinated solvents. Environ Health Persp 103:101–105.

Semprini L, Roberts PV, Hopkins GD, McCarty PL. 1990. A field evaluation of in-situ biodegradation of chlorinated ethenes: part 2. The results of biostimulation and biotransformation experiments. Ground Water 28:715–727.

Silverman RB. 1988. Mechanism-based enzyme inactivation: chemistry and enzymology, vol. 1. Boca Raton, FL: CRC Press.

Strand SE, Bjelland MD, Stensel HD. 1990. Kinetics of chlorinated hydrocarbon degradation by suspended cultures of methane-oxidizing bacteria. Res J Water Pollution Control Fed 62:124–129.

van Hylckama Vlieg, JET, de Koning W, Janssen DB. 1997. Effect of chlorinated ethene conversion on viability and activity of *Methylosinus trichosporium* OB3b. Appl Environ Microbiol 63:4961–4964.